論文

Behavior and Load Carrying Mechanism of Larger Span RC Bridge Decks: Further Exploitation of the Arching Action

Samitha JAYAKODY[*1], Atsuhiko MACHIDA[*2], Tomio YASUOKA[*3], Sayaka TAKAHASHI[*4]

ABSTRACT: The internal arching action in slabs of girder bridges due to external confinement is generally recognized. A steel free deck slab system that eliminates the need for tensile reinforcement for shorter spans is still in its conceptual stages. This paper presents the results of static tests from two scaled laboratory models. The main model was designed considering the phenomena of enhanced load carrying capacity due to external straps and internal tensile reinforcement. The second model represented only the former aspect. Both slabs that were tested failed in punching shear, and the first specimen exhibited a significant enhancement in ultimate load carrying capacity and higher efficiency in crack control.
KEYWORDS: Girder bridges, internal arching action, lateral restraints, punching shear, steel-free decks

1.INTRODUCTION

It is recalled that in most parts of the world, concrete deck slabs of girder bridges are assumed and designed as if they act predominantly in flexure. Extensive research conducted over the past twenty years in Canada confirmed that the internal arching action could be harnessed to an optimum state where the internal reinforcements in the deck slabs can be fully eliminated as a result. The major negative aspect in a steel free deck slab is the limitation to extend its transverse span and the anticipated longitudinal crack, which propagates along the full length of the underside of the deck at mid span A new approach to investigate the behavior of a modified deck is elaborated in the following experiment with experimental evidence supported by analytical results. However, the discussion is limited to experimental results in this paper. The internal compressive membrane action, popularly referred to as arch action is sustained by lateral confinements dominantly contributed due to transverse strap system that is illustrated in Figure 1. The longitudinal confinement to the deck is mainly provided by connecting the slabs to the beams by means of shear connectors.

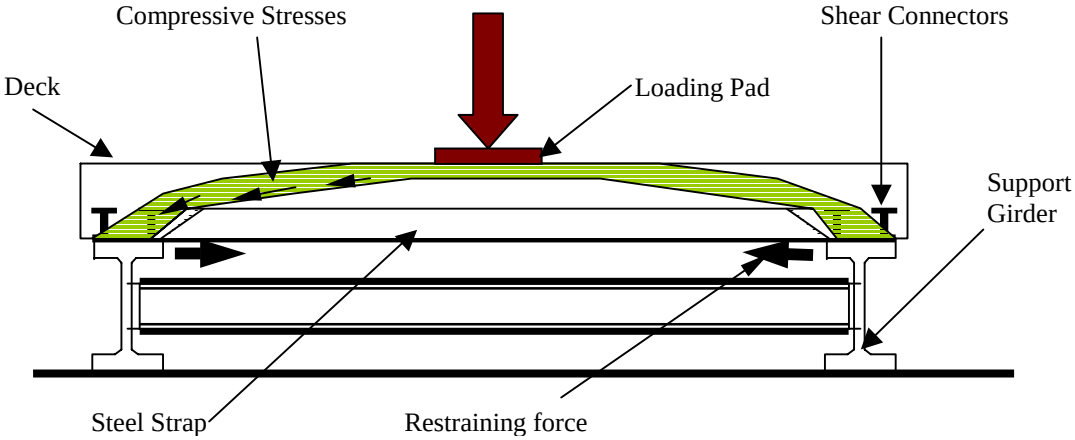

Fig.1. Compressive membrane action in deck slabs

[*1] Graduate School of Science & Engineering, Saitama University. Member, JCI
[*2] Department of Civil & Environmental Engineering, Saitama University. Professor, Member, JCI
[*3] Graduate School of Science & Engineering, Saitama University. Member, JCI
[*4]Department of Civil & Environmental Engineering, Saitama University. Undergraduate student

2.EXPERIMENTAL PROGRAM

The experimental program to investigate the behavior of the proposed deck slab system was consisted of testing and behavior monitoring of two deck slab models. They were referred to as the main specimen and the control specimen. Both of these ¼ scaled models consisted of a common main frame on which a concrete slab was placed as shown in Figures 2(a), 2(b) and represent a 6m-prototype transverse span of main girders. The main features of each model are described below.

2.1 Specimen details

2.1.1 Main and Control Specimen details

The main specimen consists of a concrete deck of 100 mm thick, cast on one of the two main frames. It also included a constant haunch of 30 mm over the girders to facilitate a separation in-between deck slab bottom and external straps. As illustrated in the Figure 2(b), external straps of 130x8 mm cross-sections were adequately connected to main girders at 750 mm intervals. Most importantly, the main model consists of internal reinforcement with 10 mm bars placed at 75 mm intervals in transverse direction and 6 mm bars placed at 100 mm intervals along longitudinal direction. Almost all the parameters and provisions of the control specimen are equal to the main specimen but completely devoid of internal reinforcements.

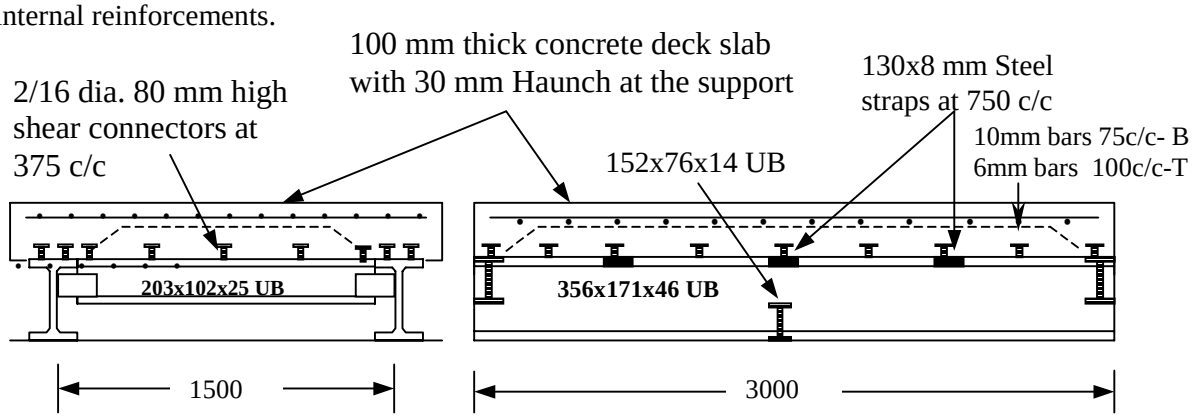

Fig. 2(a). Transverse elevation

Fig. 2(b). Longitudinal elevation (All dimensions - mm)

2.1.2 Materials

The target characteristic compressive strength of the concrete was selected as 30 MPa with max. aggregate size of 20 mm. And the average crushing strength was 34 N/mm^2. The straps were made out of steel with yield stress of 230 N/mm^2 (Grade 50). The main specimen was provided with reinforcement of average yield strength of 380 N/mm^2. E_c (mean)=25 kN/mm^2 and E_s=205 kN/mm^2.

2.2 Test arrangements and testing

Fig. 2(c). Overall support frame for main frame

Fig. 2(d). Overall view of a specimen during testing

Fig. 2(e). Loading cell with the loading pad

The instrumentation was adjusted to verify the focus of the experiment. Among the data of interest were deflections of the slab, crack and failure loads of the slab, strain in concrete and steel members. Dial gauges were placed at strategic locations to record the vertical deflection of the slab. Strain gauges were used to monitor the strain in steel elements and concrete, respectively. Strain in concrete, both top and bottom and internal reinforcements were measured at each grid points illustrated in Figure 3.

During the loading at a particular section, the displacements related to positions correspond to A, B and C were measured using displacement transducers. Figure 2c shows the main frame in association with overall supporting arrangement while Figure 2(d) and 2(e) show a typical loading arrangement for the slab system.

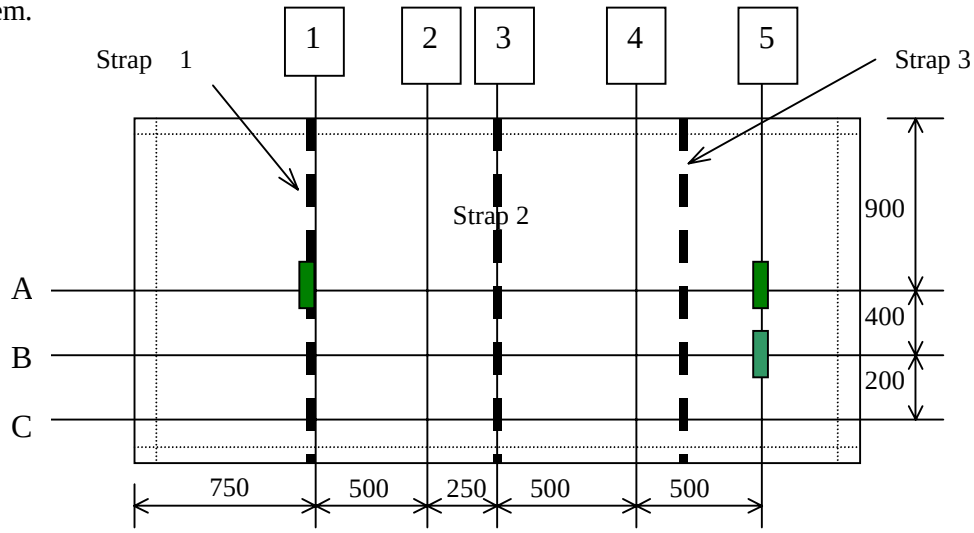

Fig 3. Plan view of a specimen and loading locations (B5 only for control specimen)

The concentrated load was generated incrementally by means of a hydraulic jack with a capacity of 1000 kN per 300 mm, connected to a steel frame. The load was applied through a 125x50 mm and 18 mm thick steel block placed on an 8 mm thick rubber pad to simulate a nominal wheel print. Two destructive tests were conducted on the main specimen at A1 and A5 locations shown in Figure 3. Similarly, on the control specimen was also subjected to two destructive tests at A1 and B5 (B5 was selected to observe the edge stiffening effect both at the end and side ways even without int. steel). During A5 and B5 loading strap no 1 and 2 were removed leaving only the middle strap in the system.

3. TEST RESULTS AND DISCUSSION

Both models described above were tested to observe the behavior in the elastic state as well as the ultimate states as stated in the figure 3.The recorded results and analyzed data from the destructive test program were tabulated in summarized form in the Table 1.Very importantly in the main specimen, the ultimate load carrying capacity and load corresponds to first crack have been improved by approximately 45% and 35% respectively compared to that of corresponding control specimen values.

Table 1: Summary of test results

Specimen	Load Positi-on	Modifications	Load (kN)		Maximum Deflection of the slab (mm)	Basic Factor of Safety		Mode of Failure
			1st Crack	Failure		Serv.	Ult.	
Main Specimen	A1	-	55(880)	205(3280)	4.42(18)	6	23	P.S*.
	A5	Without straps 1 and 3	45(720)	180(2880)	8.12(33)	5	20	P.S*.
Control Specimen	A1	-	20(320)	115(1840)	12.78(51)	2.2	13	P.S.
	B5	Without straps 1 and 3	28(448)	130(2080)	8.16(33)	3	14	P.S.

( )-Prototype values, P.S*-Very localized Punching Shear, P.S-Punching Shear

3.1 Serviceability limit, Ultimate load, Failure mode and Crack pattern

The deck slab of main model was tested to fail under a central load at two separate points, A1 and A5 as illustrated in Figure 3. Under concentrated load, the failure mode of both the location of the deck is punching shear. At A1, the first hair crack was recorded at 55 kN and thereafter started to propagate in the radial directions. The crack propagations towards the middle strap were significantly

predominant as shown in Figure 4(a). It was concluded that the behavior was due to the additional stiffening effect by the edge beam. The ultimate load was recorded as 205 kN associated with very localized punching shear. The crack patterns of both top and bottom are shown in figure 4(a) and 4(c).

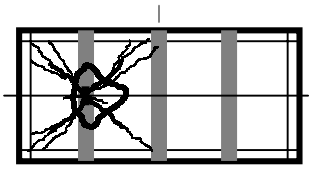

Fig.4a. Main specimen bottom cracks during A1 loading

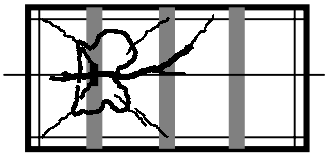

Fig.4b. Control specimen bottom cracks during A1 loading

The prototype values corresponding to serviceability and ultimate state are 880 kN and 3280 kN respectively. The maximum specified basic wheel load as per AASHTO is 145 kN for commercial vehicles. Thus according to the maximum ever design load, the observed results represent basic factors of safety approximately 6 and 23. At A5 on main specimen the slab system was modified before loading by removing two out of three steel straps, leaving only the middle strap.The recorded data was summarized in the Table 1. The rate of crack propagation and number of cracks were much higher than A1 with micro cracks. The control specimen was also subjected to the same loading positions with the same conditions as per main specimen for mere comparison, however instead of A5, the location B5 was selected to study the eccentric loading and the effect of edge stiffening. The appropriate values are shown in the table1. A significantly dominant longitudinal crack (not due to Shrinkage effect) was appeared underneath the slab while A1 loading (45 days after casting) and illustrated in Figure 4(b) and 4(d) shows the top view after failure.

Fig. 4(c). Controlled punching shear failure of main specimen

Fig .4(d). Top view of punching shear failure, Control specimen-A1

Fig. 4(e). Punching shear failure, Control specimen-B5

3.2 Loads vs Maximum Deflection of the Deck slab Relationship

As shown in Figure 5(a) and 5(b), all the graphs correspond to a region where the deflection is linearly proportional to the load increments. The maximum vertical deflection per each loading was recorded at the place of the loading. Especially in the case of A1 loading of the main specimen, the slope exhibits a slight deviation beyond 55 kN. Also the first visible crack was observed at this load and considered as the serviceability limit. The rate of deterioration of overall stiffness in this case is very small and is attributed to the enhanced rigidity of that system. However in contrary, the same load on the control specimen exhibited lesser stiffness value in the region of elastic limit and further underwent severe loss of overall stiffness of the system. In contrary, the control specimen exhibited that the elastic limit is less than the main specimen and the approximate value is recorded as 20 kN and posses less overall stiffness as well. Noticeably, just beyond 20 kN, stiffness loss was rapid up to 22 kN where there after it posses stiffness improvement up to 50 kN before it finally lost it stiffness again. This is attributed to the mobilization of lateral restraints after initial lateral deflection of the system.

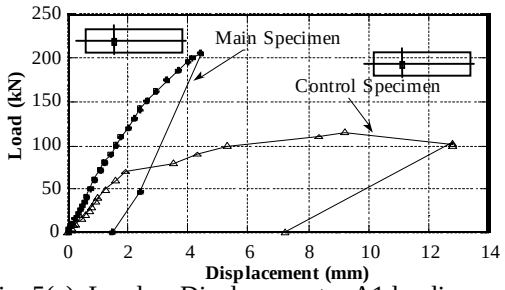

Fig 5(a) Load vs Displacement – A1 loading

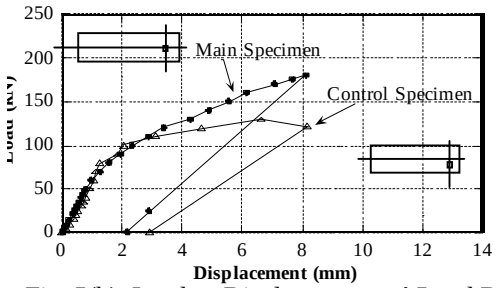

Fig 5(b) Load vs Displacement – A5 and B5

Further the A5 loading on the main specimen shows a rapid loss of stiffness due to lack of lateral restraints. However within the serviceability limits, it posses substantial rigidity due to the internal

steel which provided the initial lateral restraints and due to edge stiffening effect. The above scenario states that the inclusion of steel has very significant contribution to the system during the serviceability and contributed to the enhanced stiffness of the system. But observing the strain values mobilized in the straps it can be stated that the mobilization of the arching behavior which is based on the compressive membrane action was delayed in the maim specimen as a result of internal steel. The effect of external strap was secondary during initial loading and got dominant significantly during load increment. Thus inclusion of internal reinforcement and the lateral restraints provided by straps positively contributed to the main objectives of the study not only exhibiting enhanced load carrying capacity and controlled deflection but also increased overall stiffness. Though the edge stiffening effect has contributed to increase stiffness, the effect is considered very localized and not commonly applicable to entire slab.

3.3 Load vs Maximum compressive strain

With reference to the Figure 6(a), it can be shown that the inclusion of internal steel had a little effect on overall stiffness in the serviceability limit although the effect became dominant beyond the serviceability limit. The ultimate load carrying capacity had been enhanced by almost 80%. Further the rate of stiffness loss of the system is comparatively low due the steel inclusion and shows a more gradual change from elastic to a plastic behavior. The authors have also witnessed an increment in strain in the control specimen even after the failure, where the phenomenon is still under investigation.

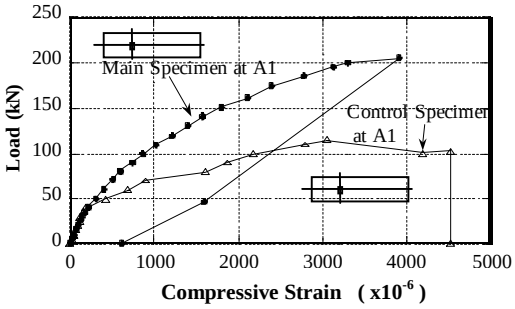

Fig. 6(a). Load vs Maximum Concrete Compressive Strain (Loading A1)

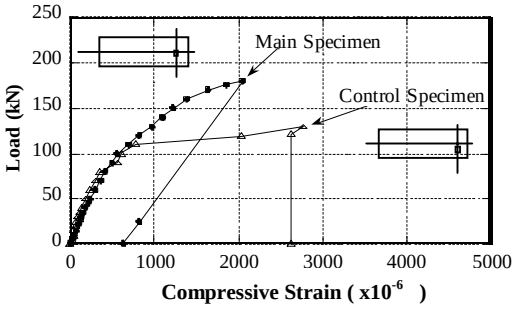

Fig. 6(b). Load vs Maximum Concrete Compressive Strain (Loading A5 & B5)

Figure 6(b) shows the significance of the edge stiffening to the overall stiffness and strength even promoting enhanced stiffness limits beyond the serviceability limits. The enhancement was due to edge stiffening and later showed a rapid deterioration. This can be attributed to the loss of edge stiffening effect after severe cracking.

3.4 Load and typical Strain behavior along the length of reinforcement

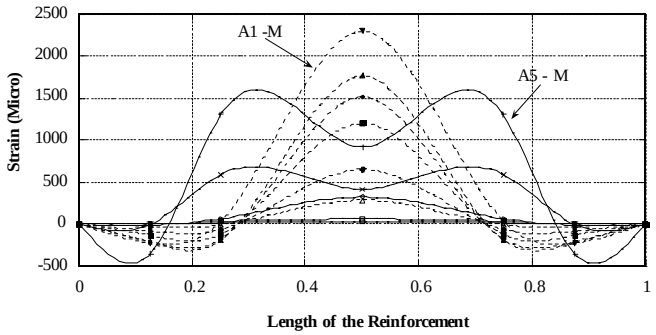

Fig. 7. Strain Behaviors in a Reinforcement Bar

It can be seen in Figure7 that the strain behavior of a steel bar in the main specimen shown significant different features during A1 loading and that of A5.The shape of the curve is supported by analytical method reported elsewhere (Jayakody and Machida 2003). The dotted lines represent the strain properties during A1. Each line corresponds to particular selected load value and upper the lines, higher the load values. The solid lines are representing A5 loading which is only with the middle strap as described earlier. The topmost lines for each case show the behavior at failure.

The behavior of strain in internal steel of A1 loading in the elastic range was exhibited that the middle one third was in tension and as it approaches towards the edge it became compressive.
Further the highest tension value corresponded to the mid span and compressive strain near the edges reiterates that the effect of arching and flexural enhancements. It was also revealed that when the load increases towards ultimatum the tensile and compressive strains increase proportionately and regions

approximately confirmed to middle and edge one thirds.In contrary to the above, during A5 loading the strain was tensile along most of the length and compressive region was limited to only about 1/8 of the span from the both edges in the elastic region and of relatively low values. When the load approaches higher values, the maximum tensile strains were reported at two points approximately at one thirds of the transverse span and the compressive region and values were increasing at a significant rate. This behavior is attributed to the edge stiffening and dominant flexural behavior in the elastic region and later activated the dowel action of internal steel when it reaches the ultimate values. Further the lines corresponds to load values of 25, 50, 75, 100,125, 150 for both cases and finally 175 for A5 and 205 for A1 case in kN.

3.5 Load carrying Mechanism

It can be summarized that the additional load carrying capacity of the proposed deck is attributed to the mechanism of compressive membrane action. This three dimensional equilibrium action occurs as a result of in-plane restraints that restrict the horizontal expansion of the bridge deck, as it deflects vertically. The transverse expansions are restricted by the internal steel and steel straps. Concurrently on the longitudinal direction by panel joint's composite action. This induces a compressive force within the slab, which increases its stiffness and strength. The internal steel contributes more significantly in both the serviceability limits and beyond the overall system except the edge stiffening that is considered to be localized and not common to the entire structure. The ultimate failure mode and behavior of the system is influenced by combined contributions from all above-mentioned factors.

4.CONCLUSIONS

The paper presented the result of an experimental study on the effects of enhanced load carrying capacity due to external straps and internal steel for larger transverse bridge spans on girder bridges. The study concluded the followings:

1. The present study verifies earlier finding that under a static concentrated load, the failure mode of the steel free deck is punching shear, moreover not flexure even with for larger spans.
2. This experiment revealed that the primary action by which these slabs resist against applied wheel is a three dimensional stress equilibrium phenomena referred to as internal arching action, where deck slabs tend to fail in a punching shear mode at a much higher load than that traditionally predicted by flexural analysis.
3. The new technology exploited that the phenomenon of the steel free deck slab reinforced with optimum steel exhibited a significant enhancement in load carrying capacity and higher efficiency in crack control by approximately 45% and 35% respectively (Table 1) giving a positive vision for further extension in transverse span without compromising safety and performance. The effect of edge stiffening exhibited very significant impact on load carrying capacity and crack control.
4. The inclusion of tensile reinforcement had an obvious effect on eliminating the longitudinal crack, which is considered a major problem in steel free slabs.

REFERENCES

1) Bakht, B. and Mufti, A.A., "Five steel-free deck slabs in Canada", *Struc. Eng. Int'l.*,N.3,1998, pp. 196-200.
2) Bakht, B., "Revisiting arching in deck slabs", *Can. J. Civ. Eng.*, Vol. 23,1996, pp. 973-981.
3) Mufti, A.A., Jaeger, L.G., Bakht, B. and Wagner, L.D., 1993.,"Experimental investigation of FRC deck slabs without internal steel reinforcement", *Can. J.Civ.Eng.*,Vol. 20, No. 3, pp.398-406.
4) Bakht, B. and Lam, C., "Behavior of transverse confining systems for Steel-Free Deck Slabs", *J. of Bridge Eng.*, May 2000, pp 139-147.
5) Mufti, A., Bakht, B. and Jaeger, L.G., "Bridge Superstructures (New Development)", National Book Foundation, Islamabad, 1996, pp. 113-159.
6) Jayakody, S. and Machida, A., "FEM analysis of Larger span RC bridges", *JSCE Summer Symp.* 2003